

## Evaluation of the LEP centre-of-mass energy above the W-pair production threshold

The LEP Energy Working Group

A. Blondel<sup>1</sup>, M. Bøege<sup>2a</sup>, E. Bravin<sup>2</sup>, P. Bright-Thomas<sup>2b</sup>, T. Camporesi<sup>2</sup>, B. Dehning<sup>2</sup>,  
M. Heemskerk<sup>2</sup>, M. Hildreth<sup>2</sup>, M. Koratzinos<sup>2</sup>, E. Lançon<sup>3</sup>, G. Mugnai<sup>2</sup>, A. Müller<sup>2,4</sup>,  
E. Peschardt<sup>2</sup>, M. Placidi<sup>2</sup>, N. Qi<sup>2c</sup>, G. Quast<sup>4</sup>, P. Renton<sup>5</sup>, F. Sonnemann<sup>2</sup>,  
E. Torrence<sup>2</sup>, A. Weber<sup>6</sup>, P. S. Wells<sup>2</sup>, J. Wenninger<sup>2</sup>, G. Wilkinson<sup>2</sup>

<sup>1</sup>Laboratoire de Physique Nucléaire et des Hautes Energies, Ecole Polytechnique, IN<sup>2</sup>P<sup>3</sup>-CNRS,  
F-91128 Palaiseau Cedex, France

<sup>2</sup>CERN, European Organisation for Particle Physics, CH-1211 Geneva 23, Switzerland

<sup>3</sup>CEA, DAPNIA/Service de Physique des Particules, CEA-Saclay, F-91191 Gif-sur-Yvette Cedex, France

<sup>4</sup>Institut für Physik, Universität Mainz, D-55099 Mainz, Germany

<sup>5</sup>Department of Physics, University of Oxford, Keble Road, Oxford OX1 3RH, UK

<sup>6</sup>Aachen I (RWTH), I. Physikalisches Institut, Sommerfeldstrasse, Turm 28, D-52056 Aachen, Germany

<sup>a</sup>Now at: PSI - Paul Scherrer Institut, Villigen, Switzerland

<sup>b</sup>Now at: School of Physics and Astronomy, University of Birmingham, Birmingham B15 2TT, UK

<sup>c</sup>Now at: Institute of High Energy Physics, Academia Sinica, P.O. Box 918, Beijing, China

### Abstract

Knowledge of the centre-of-mass energy at LEP2 is of primary importance to set the absolute energy scale for the measurement of the W-boson mass. The beam energy above 80 GeV is derived from continuous measurements of the magnetic bending field by 16 NMR probes situated in a number of the LEP dipoles. The relationship between the fields measured by the probes and the beam energy is calibrated against precise measurements of the average beam energy between 41 and 55 GeV made using the resonant depolarisation technique. The linearity of the relationship is tested by comparing the fields measured by the probes with the total bending field measured by a flux loop. This test results in the largest contribution to the systematic uncertainty. Several further corrections are applied to derive the the centre-of-mass energies at each interaction point. In addition the centre-of-mass energy spread is evaluated. The beam energy has been determined with a precision of 25 MeV for the data taken in 1997, corresponding to a relative precision of  $2.7 \times 10^{-4}$ . This is small in comparison to the present uncertainty on the W mass measurement at LEP. However, the ultimate statistical precision on the W mass with the full LEP2 data sample should be around 25 MeV, and a smaller uncertainty on the beam energy is desirable. Prospects for improvements are outlined.

# 1 Introduction

The centre-of-mass energy of the large electron-positron (LEP) collider increased to 161 GeV in 1996, allowing  $W$ -pair production in  $e^+e^-$  annihilation for the first time. This marked the start of the LEP2 programme. The energy has been further increased in a series of steps since then. A primary goal of LEP2 is to measure the  $W$ -boson mass,  $M_W \approx 80.4$  GeV. The beam energy sets the absolute energy scale for this measurement, leading to an uncertainty of  $\Delta M_W/M_W \approx \Delta E_{\text{beam}}/E_{\text{beam}}$ . With the full LEP2 data sample, the statistical uncertainty on the  $W$  mass is expected to be around 25 MeV. To avoid a significant contribution to the total error, this sets a target of  $\Delta E_{\text{beam}}/E_{\text{beam}} \approx 10^{-4}$ , i.e. 10 to 15 MeV uncertainty for a beam energy around 90 GeV. This contrasts with LEP1, where the  $Z$  mass was measured with a total relative uncertainty of about  $2 \times 10^{-5}$  [1].

The derivation of the centre-of-mass energy proceeds in several stages. First, the average beam energy around the LEP ring is determined. The overall energy scale is normalised with respect to a precise reference in occasional dedicated measurements during each year's running. Time variations in the average beam energy are then taken into account. Further corrections are applied to obtain the  $e^+$  and  $e^-$  beam energies at the four interaction points, and the centre-of-mass energy in the  $e^+e^-$  collisions. These procedures are elaborated below.

At LEP1, the average beam energy was measured directly at the physics operating energy with a precision of better than 1 MeV by resonant depolarisation (RD)[1]. The spin tune,  $\nu$ , determined by RD, is proportional to the beam energy averaged around the beam trajectory:

$$\nu = \frac{g_e - 2}{2} \frac{E_{\text{beam}}}{m_e c^2} \quad (1)$$

Both  $\nu$  and  $E_{\text{beam}}$  are also proportional to the total integrated vertical magnetic field,  $B$ , around the beam trajectory,  $\ell$ :

$$E_{\text{beam}} = \frac{e}{2\pi c} \oint_{\text{LEP}} B \cdot d\ell \quad (2)$$

Unfortunately, the RD technique can not be used in the LEP2 physics regime, because depolarising effects increase sharply with beam energy, leading to an insufficient build up of transverse polarisation to make a measurement. In 1997, the highest energy measured by RD was 55 GeV.

The beam energy in LEP2 operation is therefore determined from an estimate of the field integral derived from continuous magnetic measurements by 16 NMR probes situated in some of the 3200 LEP main bend dipoles. These probes are read out during physics running and RD measurements, and they function at any energy above about 41 GeV. Although they only sample a small fraction of the field integral, the relation between their readings and the beam energy can be precisely calibrated against RD measurements in the beam energy range 41 to 55 GeV.

The relation between the fields measured by the NMR probes and the beam energy is assumed to be linear, and to be valid up to physics energies. Although the linearity can only be tested over a limited range with the RD data themselves, a second comparison of the NMR readings with the field integral is available. A flux loop is installed in each LEP dipole magnet, and provides a measurement of 96.5% of the field integral. Flux loop experiments are performed only occasionally, without beam in LEP. The change in flux

is measured during a dedicated cycling of the magnets. The local dipole bending fields measured by the NMR probes are read out at several steps in the flux-loop cycle, over the full range from RD to physics energies. This provides an independent test of the linearity of the relation between the probe fields and the total bending field.

The use of the NMR probes to transport the precise energy scale determined by RD to the physics operating energy is the main novelty of this analysis. The systematic errors on the NMR calibration are evaluated from the reproducibility of different experiments, and the variations from probe to probe. The dominant uncertainty comes from the quality of the linearity test with the flux loop.

At LEP2, with 16 NMR probes in the LEP tunnel, time variations in the dipole fields provoked by leakage currents from neighbourhood electric trains and due to temperature effects can be accounted for directly. This is in contrast to the LEP1 energy measurement, where understanding the time evolution of the dipole fields during a LEP fill formed a major part of the analysis [1].

The NMR probes and the flux loop measure only the magnetic field from the LEP dipoles, which is the main contribution to the field integral. The LEP quadrupoles also contribute to the field integral when the beam passes through them off axis, which occurs if for any reason the beam is not on the *central orbit*. The total orbit length is fixed by the RF accelerating frequency. Ground movements, for example due to earth tides or longer time scale geological effects, move the LEP magnets with respect to this fixed orbit [1]. At LEP2, deliberate changes in the RF frequency away from the nominal central value are routinely used to optimise the luminosity by reducing the horizontal beam size. This can cause occasional abrupt changes in the beam energy. Orbit corrector magnets also make a small contribution to the total bending field. All of these corrections must be taken into account both when comparing the NMR measurements with the RD beam energies, and in deriving the centre-of-mass energy of collisions as a function of time.

The exact beam energy at a particular location differs from the average around the ring because of the loss of energy by synchrotron radiation in the arcs, and the gain of energy in the RF accelerating sections; the total energy lost in one revolution is about 2 GeV at LEP2. The  $e^+$  and  $e^-$  beam energies at each interaction point are calculated taking into account the exact accelerating RF configuration. The centre-of-mass energy at the collision point can also be different from the sum of the beam energies due to the interplay of collision offsets and dispersion. The centre-of-mass energies for each interaction point are calculated every 15 minutes, or more often if necessary, and these values are distributed to the LEP experiments.

In the following section, the data samples and magnetic measurements are described. The beam energy model is outlined in section 3. The calibration of the NMR probes and the flux-loop test are described in section 4. More information on corrections to the beam energy from non-dipole effects is given in section 5, and on IP specific corrections to derive the centre-of-mass energy in section 6. The systematic uncertainties for the whole analysis are summarised in section 7. The evaluation of the instantaneous spread in centre-of-mass energies is given in section 8. In the conclusion, the prospects for future improvement are also outlined.

## 2 Data samples

## 2.1 Luminosity delivered by LEP2

LEP has delivered about  $10 \text{ pb}^{-1}$  at each of two centre-of-mass energies, 161 and 172 GeV, in 1996, and over  $50 \text{ pb}^{-1}$  at a centre-of-mass energy of around 183 GeV in 1997. Combining the data from all four LEP experiments, these data give a measurement of the W mass with a precision of about 90 MeV [2]. This paper emphasises the 1997 energy analysis, with some information for 1996 where relevant.

## 2.2 Polarisation measurements

Date	Fill	41 GeV	44 GeV	50 GeV	55 GeV	Optics
19/08/96	3599			yes		90/60
31/10/96	3702		yes			90/60
03/11/96	3719		yes	yes		90/60
17/08/97	4000		yes			90/60
06/09/97	4121		yes	yes		60/60
30/09/97	4237		yes	yes		60/60
02/10/97	4242	yes	yes	yes	yes	60/60
10/10/97	4274		yes			90/60
11/10/97	4279	yes	yes	yes	yes	60/60
29/10/97	4372	yes	yes			60/60

Table 1: Fills with successful polarisation measurements in 1996 and 1997. Each calibrated energy point is marked “yes”.

The successful RD experiments in 1996 and 1997 are listed in table 1. To reduce uncertainties from fill-to-fill variations, an effort was made to measure as many beam energies as possible with RD during the same LEP fill. Measuring two energies in the same fill was first achieved at the end of 1996. The need for more RD measurements motivated the “k-modulation” programme to measure the offsets between beam pickups and quadrupole centres [3], the improved use of magnet position surveys, and the development of a dedicated polarisation optics [4] (the 60/60 optics<sup>1</sup>). These were all used in 1997 [5]. Improving the orbit quality and reducing depolarising effects in this way resulted in 5 fills with more than one energy point, and 2 fills with 4 energy points, which allow a check of the assumption that the measured magnetic field is linearly related to the average beam energy. The range over which tests can be made increased from 5 to 14 GeV between 1996 and 1997, and the maximum RD calibrated energy increased from 50 to 55 GeV. At least a 4–5% level of polarisation is needed to make a reliable measurement, but only 2% level of polarisation was observed at 60 GeV in 1997.

---

<sup>1</sup>The optics are designated by the betatron advance between focusing quadrupoles of the LEP arcs in the horizontal/vertical planes respectively.

## 2.3 Magnetic measurements

The LEP dipole fields are monitored continuously by NMR probes, and in occasional dedicated measurements by the flux loop. A total of 16 probes was installed for the 1996 LEP run. The probes are positioned inside selected main bend dipoles, as indicated in figure 1. Each octant has at least one probe, and octants 1 and 5 have strings of probes in several adjacent dipoles (and in one instance two probes in the same dipole). The probes measure the local magnetic field with a precision of around  $10^{-6}$ , and they can be read out about every 30 seconds. Each probe only samples the field in a small region of one out of 3200 dipoles. A steel field plate is installed between each probe and the dipole yoke to improve the uniformity of the local magnetic field. During normal physics running and RD measurements, the probe readings over five minute time intervals are averaged. This reduces the effect of fluctuations in the magnetic fields induced by parasitic currents on the beam pipe (see section 3). The probes are also read out during flux-loop measurements, as described below.

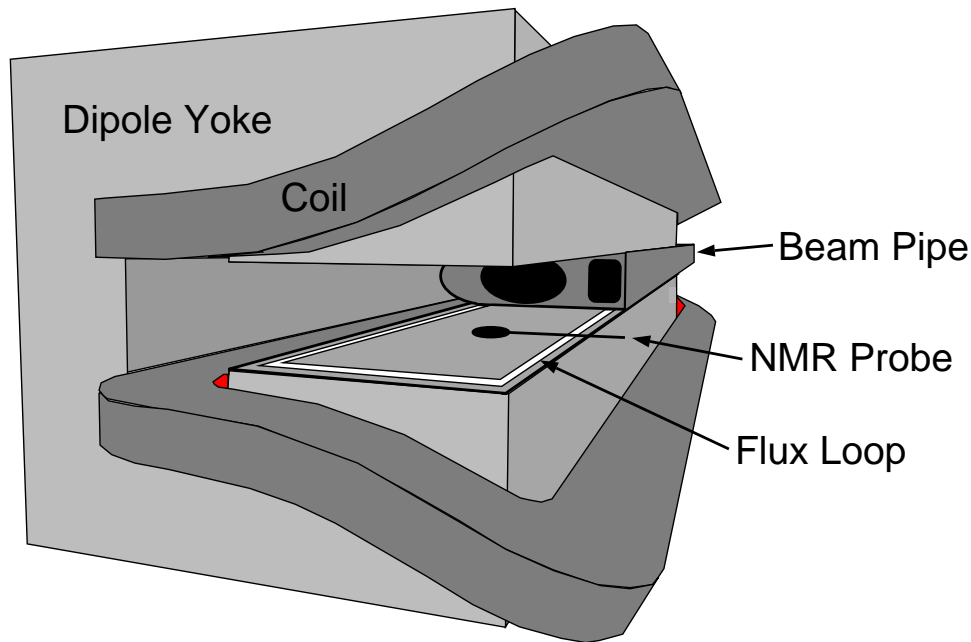


Figure 1: A LEP dipole magnet showing the flux loop and an NMR probe.

In 1995 there were only two probes in dipoles in the LEP ring, and prior to 1995, only a reference magnet powered in series with the main dipoles was monitored [1]. The larger number of available probes in 1996 and 1997 has allowed a simplification of the treatment of the dipole magnetic field evolution during a fill (see section 3).

The performance of the probes is degraded by synchrotron radiation at LEP2. A new probe gives a strong enough signal to lock on to and measure for fields corresponding to beam energies above about 40 GeV. During a year's running, this minimum measurable field gradually increases, and the probes eventually have to be replaced. However, if a stable frequency lock is achieved, then the value of the field measured is reliable; only the range of measurable fields is compromised. During 1996 and 1997, all of the probes were working at high energy, with the exception of two probes, one in each multi-probe octant, which were not available for the running at 172 GeV centre-of-mass energy.

The flux loop is also shown schematically in figure 1. In contrast to the NMR probes, the flux loop samples 98% of the field of each main bend dipole, excluding fringe fields at the ends, corresponding to 96.5% of the total bending field of LEP. The loop does not include the weak (10% of normal strength) dipoles at the ends of the arcs, the double-strength dipoles in the injection regions, or other magnets such as quadrupoles or horizontal orbit correctors.

The flux loop measures the change in flux during a dedicated magnet cycle, outside physics running, and the corresponding change in the average main dipole bending field,  $B_{\text{FL}}$ , is calculated. Five of these measurements were made in 1997. The gradual increase of the magnetic field during the cycle is stopped for several minutes at a number of intermediate field values, each of which corresponds to a known nominal beam energy, to allow time for the NMR probes to lock and be read out. The values chosen include the energies of RD measurements and physics running. The average of the good readings for each probe is calculated for each step. These special flux-loop measurements are referred to by an adjacent LEP fill number (one measurement in fills 4000, 4121 and 4206 and two measurements in fill 4434). This possibility to cross-calibrate the field measured by the flux loop and by the NMR probes is crucial to the analysis.

### 3 The beam energy model

The LEP beam energy is calculated as a function of time according to the following formula:

$$\begin{aligned}
 E_{\text{beam}}(t) = & (E_{\text{initial}} + \Delta E_{\text{dipole}}(t)) \\
 & \cdot (1 + C_{\text{tide}}(t)) \cdot (1 + C_{\text{orbit}}) \cdot (1 + C_{\text{RF}}(t)) \\
 & \cdot (1 + C_{\text{h.corr.}}(t)) \cdot (1 + C_{\text{QFQD}}(t)).
 \end{aligned}
 \tag{3}$$

The first term,  $E_{\text{initial}}$ , is the energy corresponding to the dipole field integral at the point when the dipoles reach operating conditions, i.e. after the beams have been “ramped” up to physics energy, and after any bend modulation has been performed (see below). For RD fills,  $E_{\text{initial}}$  is calculated after each ramp to a new energy point. The shift in energy caused by changes in the bending dipole fields during a fill is given by  $\Delta E_{\text{dipole}}(t)$ .

Both of these “dipole” terms are averages over the energies predicted by each functioning NMR probe. For the initial energy, equal weight is given to each probe, since each gives an independent estimate of how a magnet behaves as the machine is ramped to physics energy. However, for the change in energy during a fill, equal weight is given to each octant. This gives a more correct average over the whole ring for dipole rise effects provoked by temperature changes, and by parasitic electrical currents on the beam pipe caused by trains travelling in the neighbourhood.

Modelling the dipole energy using the 16 NMR probes has simplified the treatment compared to LEP1, where only two probes were available in the tunnel in 1995, and none in earlier years. For LEP1,  $E_{\text{initial}}$  was derived from comparisons with RD measurements, and the rise in a fill from a model of the train and temperature effects (see [1]).

The dipole rise effects are minimised by bend modulation, i.e. a deliberate small amplitude variation of the dipole excitation currents after the end of the ramp[1]. These

were not recommissioned for the 1996 running, but in 1997 were carried out routinely for physics fills from fill 3948 on 5 August.

The remaining terms correct for other contributions to the integral bending field, and are listed below. They are discussed in section 5, and in more detail in reference [1]. These terms must also all be taken into account when comparing the energy measured at a particular time by RD with the magnetic field measured in the main dipoles by the NMR probes.

$C_{\text{tide}}(t)$ : This accounts for the effect of earth tides which change the size of the LEP ring, effectively moving the quadrupole magnets with respect to the fixed-length beam orbit.

$C_{\text{orbit}}$ : This is evaluated once for each LEP fill. It corrects for distortions of the ring geometry on a longer time scale according to the measured average horizontal orbit displacement.

$C_{\text{RF}}(t)$ : Regular changes in the RF frequency away from the nominal central frequency are made to optimise the luminosity, leading to this correction.

$C_{\text{h.corr.}}(t)$ : This accounts for changes in the field integral from horizontal orbit corrector magnets used to steer the beam.

$C_{\text{QFQD}}(t)$ : Stray fields are caused when different excitation currents are supplied to focussing and defocussing quadrupoles in the LEP lattice. These are taken into account by this term.

## 4 Calibration of NMR probes

### 4.1 Calibration of NMR probes with RD measurements

The magnetic fields  $B_{\text{NMR}}^i$  measured by each NMR  $i = 1, 16$ , are converted into an equivalent beam energy. The relation is assumed to be linear, of the form

$$E_{\text{NMR}}^i = a^i + b^i B_{\text{NMR}}^i. \quad (4)$$

In general, the beam energy is expected to be proportional to the integral bending field. The two parameters for each probe are determined by a combined fit to all of the energies measured by resonant depolarisation. The NMR probes only give an estimate of the dipole contribution to the integral bending field, so all the other effects, such as those due to coherent quadrupole motion, must be taken into account according to equation 3 in order to compare with the energy measured by RD. A further complication arises because two different weighted averages over probes are used to derive  $E_{\text{initial}}$  and  $\Delta E_{\text{dipole}}(t)$ , so in practice an iterative procedure is used. The average offset,  $a$ , is 27 MeV, with an rms spread over 16 NMR probes of 64 MeV. The average slope,  $b$ , is 91.17 MeV/Gauss, with an rms spread of 0.25 MeV/Gauss over 16 probes.

The residuals,  $E_{\text{pol}} - E_{\text{NMR}}^i$ , are examined for each NMR. The residuals evolve with beam energy in a different way for different probes, but for a particular probe this behaviour is reproduced from fill to fill. The residuals averaged over NMR probes at each polarisation point are shown in figure 2(a), in which the errors are displayed as the rms/ $\sqrt{N}$ ,

where  $N \leq 16$  is the number of NMR probes functioning for the measurement. This figure shows the average residuals with respect to the simultaneous fit to all polarisation fills in 1997, which was used to calibrate the NMR probes. In figure 2(b), the residuals for the two fills with four RD energies are shown. Here the fit is made to each fill individually. The residuals show a reproducible small but statistically significant deviation from zero, with the 45 and 50 GeV points being a few MeV higher than those at 41 and 55 GeV. Despite some fill-to-fill scatter, this shape is present in all fills, not just the two fills with four RD energies.

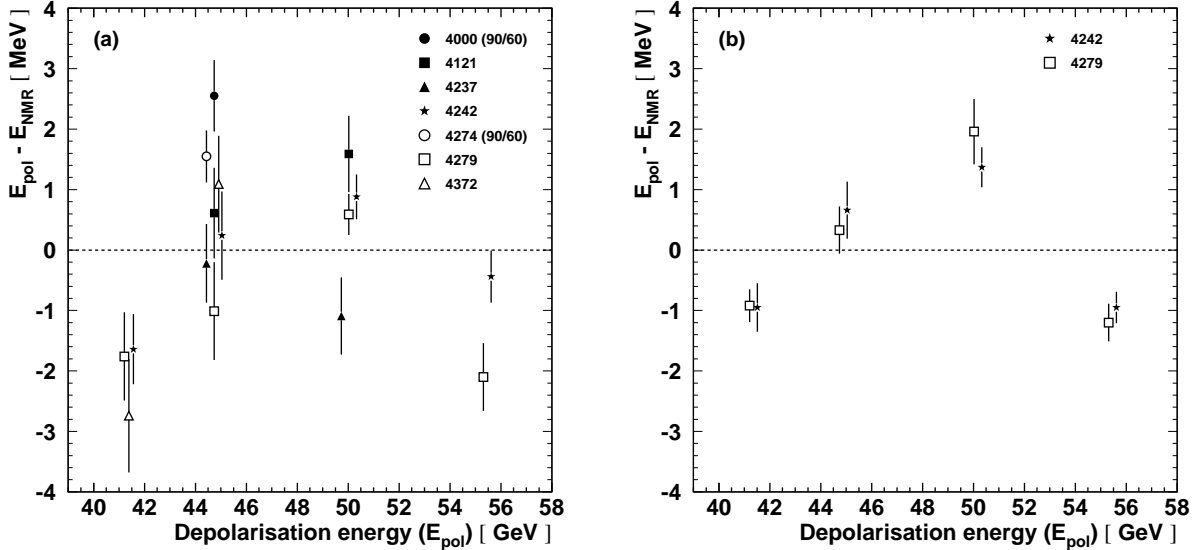


Figure 2: Residuals of the fit comparing RD energies to the energies predicted by the model (a) for a simultaneous fit to all fills and (b) for individual fits to each four point fill. For clarity, the points for different fills have been plotted at slightly displaced depolarisation energies.

## 4.2 Predicted energy for physics running

Using the calibration coefficients determined in section 4.1, the magnetic field measured by each NMR during physics running can be used to predict the beam energy. To assess the variations over the NMR probes, the average magnetic field is calculated for each NMR over all of the physics running at a nominal beam energy of 91.5 GeV. The average physics energies derived from these average fields have an rms scatter over the NMR probes of about 40 MeV, contributing  $40/\sqrt{16} = 10$  MeV to the systematic uncertainty from the normalisation procedure.

In 1996, the limited number of available RD measurements were fitted to a line passing through the origin,  $E_{\text{pol}} = p^i B_{\text{NMR}}^i$ . If this is tried for the 1997 data, the rms scatter increases to 60 MeV and the central value shifts by around 20 MeV. This is taken into account in evaluating the uncertainty for the 1996 data, as discussed in section 7.1. The reduced scatter for the two parameter fit can be taken to imply that a non-zero offset improves the description of the energy-magnetic field relation, or that it is an advantage



to impose the linearity assumption only over the region between polarisation and physics energies.

Using different polarisation fills as input to the procedure gives some variation. Fill 4372 has the most unusual behaviour. This is partly because it only samples the two lower energy points, which have a different average slope to the four point fills. This fill also has the smallest number of functioning NMR probes, since it is at the end of the year. It therefore has little weight in the overall average. An uncertainty of 5 MeV is assigned to cover the range of central values derived using different combinations of polarisation fills.

The average residuals of the fit show a characteristic shape which is a measure of the non-linearity in the beam energy range 41–55 GeV. The amplitude of the deviations is larger than the statistical scatter over the NMR probes. The linearity is best examined by making fits to the individual 4 point fills. If the errors are inflated to achieve a  $\chi^2/\text{dof}$  of 1, then they imply an uncertainty at physics energy of 7 MeV for the linear extrapolation. No additional uncertainty is included to account for this observation, because it is covered by the larger uncertainty assessed in section 4.5, where the linearity assumption is tested by a comparison of NMR and flux-loop measurements.

### 4.3 Initial fields for physics fills

The estimates of  $E_{\text{initial}}$ , the initial energy from the dipole contribution to the bending field, for all fills with a nominal centre-of-mass energy of 183 GeV are shown in figure 3. There is a change in initial field after 5 August, attributed to the implementation of bend modulation at the start of each fill. A small drift in the dipole excitation current for the

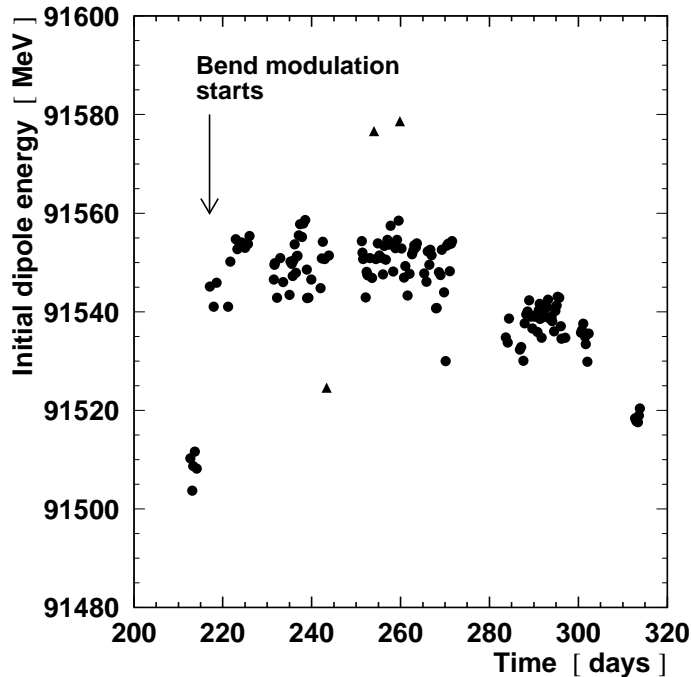


Figure 3: Initial dipole field for all 183 GeV fills. The fills marked with a triangle have anomalous initial currents in the main bend dipoles. A bend modulation was carried out at the start of each fill from 5 August (day 217).

same nominal setting was observed during the year, and one or two fills have anomalous initial values due to known incorrect setting of the excitation current. The overall rms spread in  $E_{\text{initial}}$  is 11 MeV for 148 fills. The error on the mean beam energy from these variations and from other rare anomalies at the starts of fills is taken to be 2 MeV.

#### 4.4 Uncertainty due to dipole rise

The average of the NMR probes is used to take into account changes in energy due to temperature and parasitic currents which cause the dipole bend field to change. Bend modulation [1] was not performed in 1996, but in 1997 was routinely carried out at the start of each fill from 5 August (fill 3948). The average rise in dipole field during a fill was therefore smaller in 1997 than in 1996: the total dipole rise effect on the average beam energy was only 3.5 MeV. From experience at LEP1, and the fact that the 16 NMR probes give a good sampling of the whole ring, the uncertainty is expected to be less than 25% of the effect, so 1 MeV is assigned as the uncertainty due to the dipole rise.

#### 4.5 Test of NMR calibration using the flux loop

The estimate of the integral dipole field from the NMR probes can also be compared with the measurement of 96.5% of the total bending field by the flux loop. This allows a test of the entire extrapolation method. From a fit in the 41–55 GeV region, the NMR probes can be used to predict the average bending field measured by the flux loop at the setting corresponding to physics energy. If the NMR probes can predict the flux-loop field, and the beam energy is proportional to the total bending field, then it is a good assumption that the probes are also able to predict the beam energy in physics. The flux loop can not be used to predict the beam energy in physics directly, since neither the slope nor

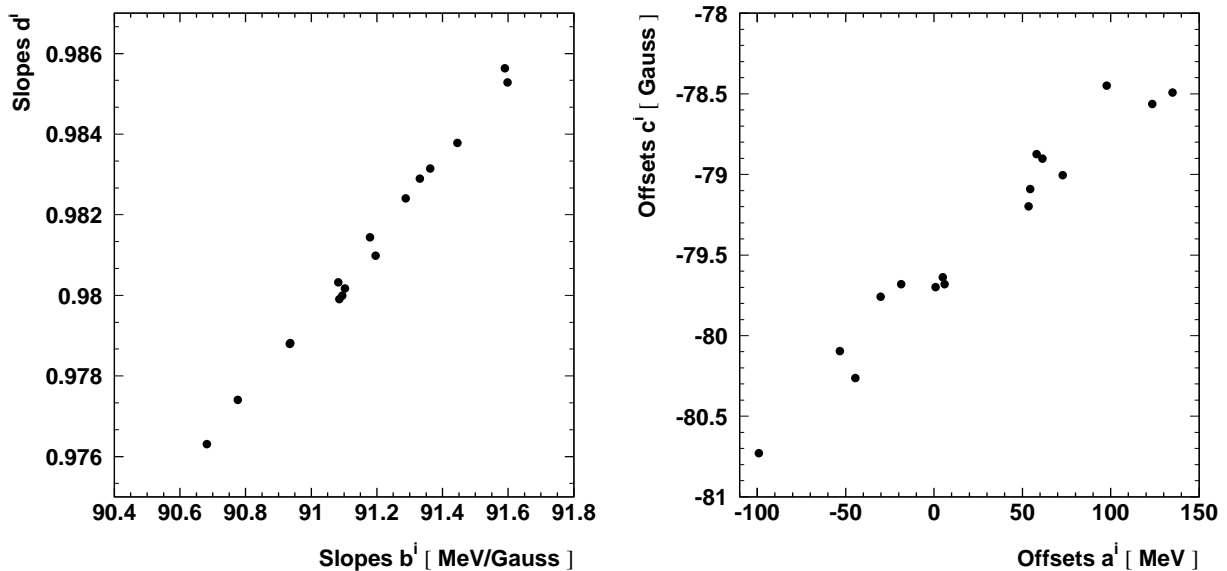


Figure 4: The slopes and offsets of equations 5 and 6 comparing the field measured by each NMR probe with the RD and flux-loop measurements. The values shown are averages over the five flux-loop measurements. There is one entry per NMR probe in each plot.

the offset of the relationship between measured field and beam energy are known with sufficient precision. However, each point in the flux loop does correspond to a specific setting of the nominal beam energy. The flux-loop measurement is from 7 to 100 GeV.

For the test to be valid, a strong correlation should be observed between the offsets  $a^i$  and  $c^i$ , and between the slopes  $b^i$  and  $d^i$ , from the fits of the field measured by each probe,  $i$ , to the polarisation and flux-loop data:

$$E_{\text{pol}} = a^i + b^i B_{\text{NMR}}^i \quad \text{and} \quad (5)$$

$$B_{\text{FL}} = c^i + d^i B_{\text{NMR}}^i \quad \text{fit restricted to 41–55 GeV.} \quad (6)$$

The fitted parameters for each NMR are shown in figure 4, and the expected correlation is seen. The average offset,  $c$ , is  $-79.38$  Gauss, with an rms spread over the 16 values of 0.67. This offset corresponds to the 7 GeV nominal beam energy setting at the start of the flux-loop cycle. The average slope,  $d$ , is 0.9811, with an rms spread over 16 NMR probes of 0.0027. The field plates cause the slope to be 2% different from unity.

The residuals with respect to equation 6 above the fit region (41–55 GeV) are used to test the linearity assumption. The residual difference in Gauss between the flux-loop and NMR fields at a particular beam energy can be converted to a residual bias in MeV by a scale factor of 92.9 MeV/Gauss (corresponding to the ratio of average slopes,  $b/d$ ).

An example fit to one flux-loop measurement is shown in figure 5. The average over the NMR probes of the scaled residuals to the fits to equation 6 are shown at each nominal beam energy. The error bars show the rms scatter divided by the square root of the number of working probes. The fit is in the range 41–55 GeV, and the error bars increase above this region. The deviations measured at the physics energy of 91.5 GeV for each of the five flux-loop measurements are shown in figure 6, using the same conventions. The probes in different magnets show a different evolution of the residuals as the nominal beam energy increases. However, for a particular magnet the behaviour is similar for each flux-loop measurement.

The average bias at physics energy is up to 20 MeV, with an rms over the probes of 30–40 MeV, corresponding to an uncertainty of 10–20 MeV depending on the number of working probes. The size of the bias tends to increase during the year; the bias becomes more negative. This is partially understood as being due to the smaller sample of NMR probes available in the latter part of the year, as is also illustrated in figure 6. To account for the correlated uncertainties from measurement to measurement, the difference in bias between the first and last measurements has been found for all of the probes that are common to the two. A significant average difference of  $-21 \pm 5$  MeV is observed, for which no explanation has been found. In fact, only the last two flux loops include a 41 GeV point, but the biases measured are not sensitive to excluding this point altogether. Other systematic effects that have been observed, for example a discrepancy of around 2 MeV if two very close by energy points are measured, are too small to explain the trend.

A detailed comparison of NMR and flux-loop data in the region of the RD measurements (41–55 GeV), shown in figure 7, reveals a different non-linearity to the NMR–polarisation comparison. However, the subset of probes included here is not exactly the same as in figure 2, and the average residuals to the flux-loop fits are only a few MeV which is at the limit of the expected precision.

The tests with the flux loop are not used to correct the NMR calibration from polarisation data, but are taken as an independent estimate of the precision of the method. A

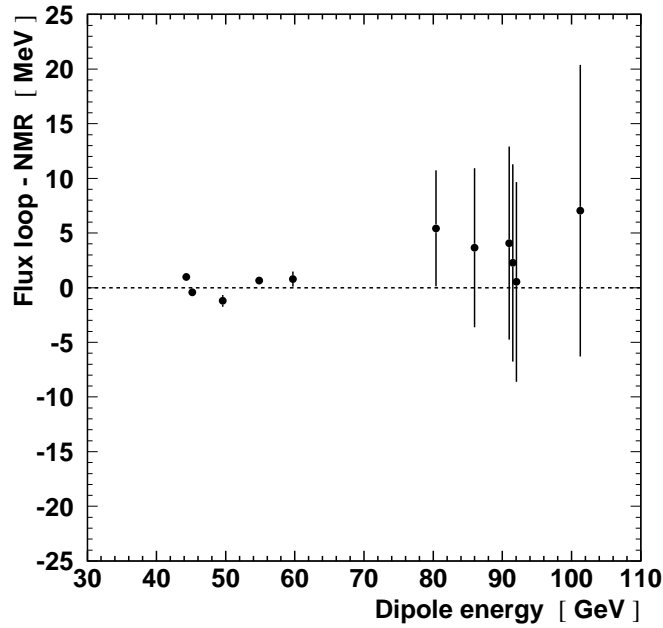


Figure 5: The difference scaled by 92.9 MeV/Gauss between the magnetic field measured by the flux loop and predicted by the NMR probes as a function of the nominal beam energy for fill 4000. The error bars give the rms scatter over the probes, divided by the square root of the number of probes.

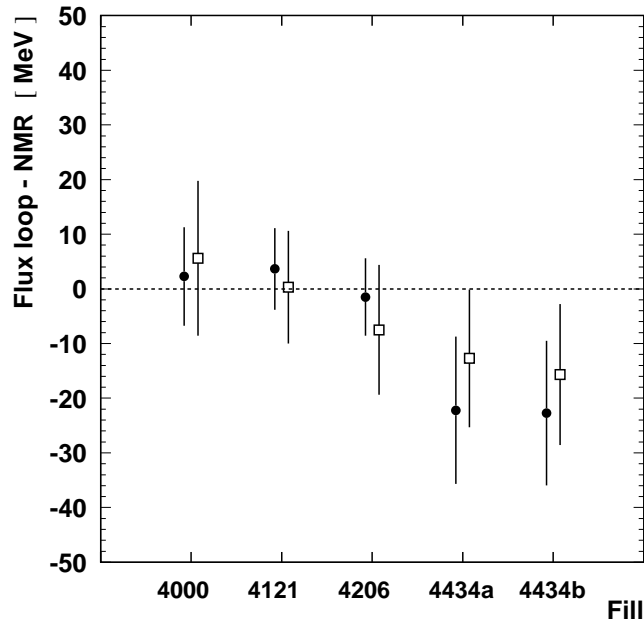


Figure 6: The difference scaled by 92.9 MeV/Gauss between the magnetic field measured by the flux loop and predicted by the NMR probes at physics energy (91.5 GeV) for each flux-loop measurement. The solid points are for all working probes for each fill, while the empty points are for the common set of probes working for all fills.

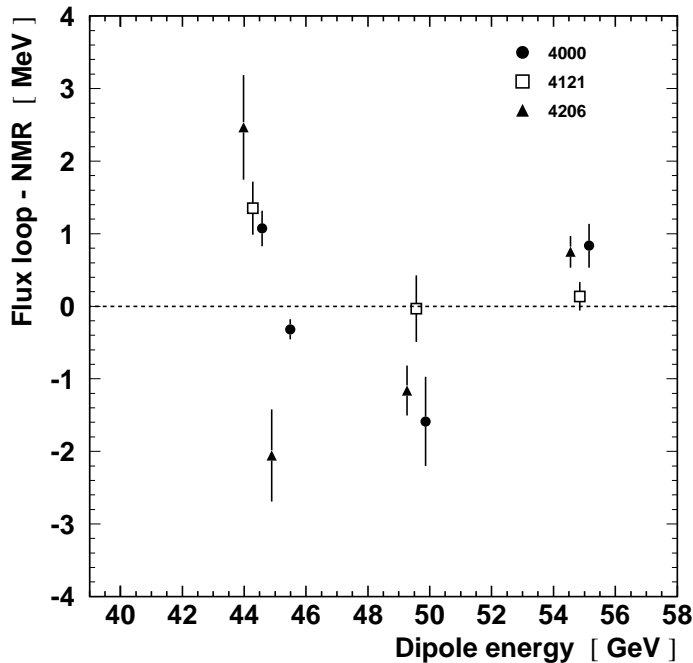


Figure 7: The residuals in the low energy region with respect to separate fits to each of the flux-loop measurements 4000,4121 and 4206, using the subset of NMR probes available at all points shown in all 3 fills. Too few NMR probes are working for all low energy points to include fill 4434 here.

systematic uncertainty of 20 MeV covers the maximum difference seen during the year. An average over the flux-loop measurements would give a smaller estimate.

#### 4.6 Uncertainty from bending field outside the flux loop

The flux loop is embedded in each of the main LEP bending dipoles, but only samples 98% of the total bending field of each dipole. The effective area of the flux loop varies during the ramp because the fraction of the fringe fields overlapping neighbouring dipoles varies. The saturation of the dipoles, expressed as the change in effective length, was measured before the LEP startup on a test stand for different magnet cycles. The correction between 45 and 90 GeV is of the order of  $10^{-4}$ , corresponding to a 5 MeV uncertainty in the physics energy.

The weak (“10%”) dipoles matching the LEP arcs to the straight sections contribute 0.2% to the total bending field. Assuming that their field is proportional to that of the main bends between RD and physics energies to better than 1%, their contribution to any non-linearity in the extrapolation is around 1 MeV.

The bending field of the double strength dipoles in the injection region contributes 1.4% of the total. Their bending field has been measured by additional NMR probes installed in the tunnel in 1998, and found to be proportional to the bending field of the main dipoles to rather better than  $10^{-3}$ , which gives a negligible additional systematic uncertainty.

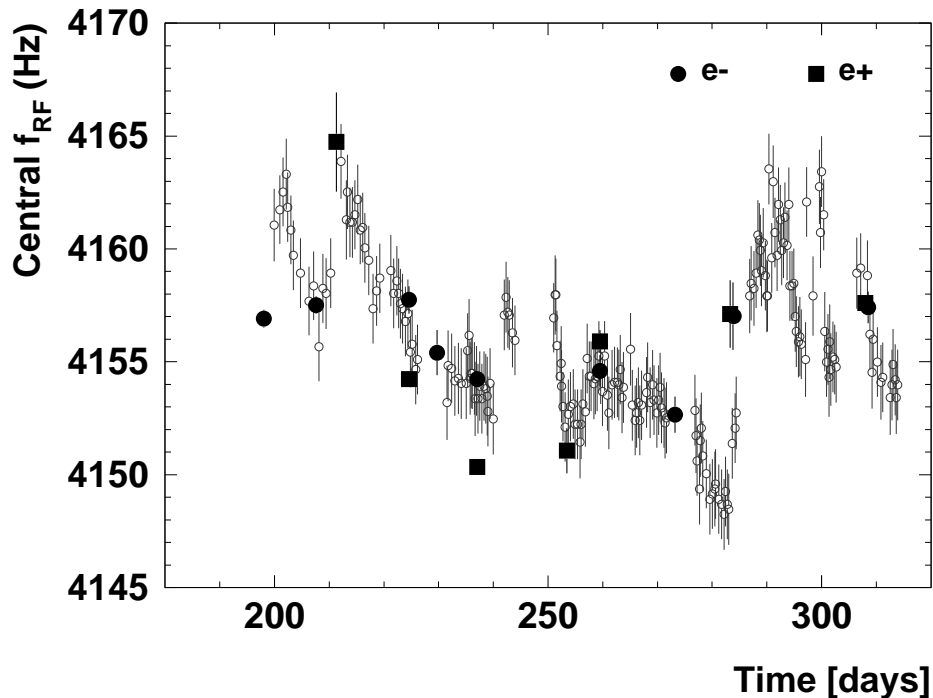


Figure 8: Evolution of the central frequency as a function of time for the 1997 LEP run. The solid points are actual  $f_c^{\text{RF}}$  measurements for  $e^-$  and  $e^+$  while the open points are obtained from  $x_{\text{arc}}$ , after correction for tides. On some occasions, the electrons and positron  $f_c^{\text{RF}}$  differ by up to 4 Hz. Note that the vertical scale shows a variation in the last four digits of the LEP RF frequency, which is nominally 352 254 170 Hz.

## 5 Quadrupole and horizontal orbit corrector effects

### 5.1 Earth tides

The model of earth tides is well understood from LEP1 [1]. It should be noted that the amplitude of the tide effect is proportional to energy, and so is larger at LEP2.

### 5.2 Central Frequency and Machine Circumference

For a circular accelerator like LEP the orbit passing on average through the centre of the quadrupoles is referred to as the *central orbit*, and the corresponding RF frequency setting is known as the *central RF frequency*  $f_c^{\text{RF}}$ . When the RF frequency  $f^{\text{RF}}$  does not coincide with  $f_c^{\text{RF}}$  the beam senses on average a dipole field in the quadrupoles, which causes a relative beam energy change  $\Delta E$  of :

$$\frac{\Delta E}{E} = -\frac{1}{\alpha} \frac{f^{\text{RF}} - f_c^{\text{RF}}}{f^{\text{RF}}} \quad (7)$$

where  $\alpha$  is the momentum compaction factor, which depends on the optics used in LEP. Its value is  $1.54 \cdot 10^{-4}$  for the 102/90 optics,  $1.86 \cdot 10^{-4}$  for the 90/60 optics and  $3.86 \cdot 10^{-4}$  for the 60/60 optics, with a relative uncertainty of  $\lesssim 1\%$ .

The central frequency is only measured on a few occasions during a year's running and requires non-colliding beams [6]. The monitoring of the central orbit and of the ring circumference relies on the measurement of the average horizontal beam position in the LEP arcs,  $x_{\text{arc}}$  [7]. As the length of the beam orbit is constrained by the RF frequency, a change in machine circumference will be observed as a shift of the beam position relative to the beam position monitors (BPMs). Figure 8 shows the evolution of the central frequency determined through  $x_{\text{arc}}$  as well as the direct  $f_c^{\text{RF}}$  measurements. The  $x_{\text{arc}}$  points have been normalised to the electrons  $f_c^{\text{RF}}$  measurements. The occasional difference of about 4 Hz between the electrons and positron  $f_c^{\text{RF}}$  (measured at physics energy) is not understood. A similar systematic effect has also been seen in 1998. Therefore a systematic error of  $\pm 4$  Hz is assigned to the central frequency. This results in an uncertainty of 1.5 MeV in the predicted difference between the energies measured by RD with the 90/60 and 60/60 optics at 45 GeV beam energy.

A correction to the energy of each fill using the measured orbit offset in the LEP arcs is applied to track the change in  $f_c^{\text{RF}}$ .

### 5.3 RF frequency shifts

For the first time in 1997, the RF frequency was routinely increased from the nominal value to change the horizontal damping partition number [9]. This is a useful technique at high energy, causing the beam to be squeezed more in the horizontal plane, and increasing the specific luminosity, whereas at lower energy, beam-beam effects prevent the horizontal beam size reduction. Less desirable side effects are that the central value of the beam energy decreases, the beam energy spread increases, and slightly more RF accelerating voltage is needed to keep the beam circulating. A typical frequency shift of +100 Hz gives a beam energy decrease of about 150 MeV. Occasionally, when an RF unit trips off, the LEP operators temporarily decrease the RF frequency to keep the beam lifetime high, in which case the beam energy values are immediately recalculated instead of waiting the usual 15 minutes.

### 5.4 Horizontal Corrector Effects

Small, independently-powered dipole magnets are used to correct deviations in the beam orbit. Horizontal correctors influence the beam energy either through a change of the integrated dipole field or through a change of the orbit length  $\Delta L_1$  [8]. In general the two effects could be mixed and cannot be easily disentangled, although simulations show that the orbit lengthening effect should dominate. For a given orbit and corrector settings, the predicted energy shifts can differ by 30% between the two models, which implies that a 30% error should be applied to the energy shifts predicted for the corrector settings.

In general the settings of the horizontal correctors are different for different machine optics, and also for different beam energies. The energy model described by equation 3 includes this optics dependent correction explicitly. RD measurements using any optics can therefore be combined when calibrating the NMR probes (section 4.1), which estimate the dominant contribution from the main bend dipoles.

For an orbit lengthening  $\Delta L_1$  the energy change is :

$$\frac{\Delta E}{E} = -\frac{\Delta L_1}{\alpha C} \quad (8)$$

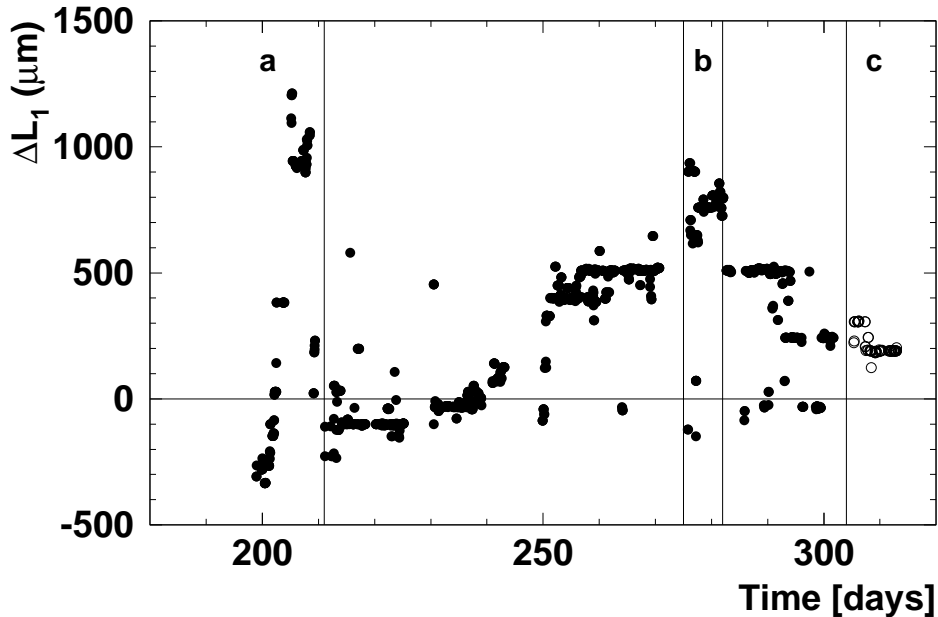


Figure 9: Evolution of the orbit lengthening  $\Delta L_1$  during the 1997 LEP run. In period (a) the beam energy is 45 GeV, in period (b) 65 and 68 GeV. In period (c) the 102/90 optics was tested at 91.5 GeV. All other data correspond to beam energies between 91 and 92 GeV with the 90/60 optics. For  $\Delta L_1 = 500 \mu m$ , the energy shift is about 11 MeV at 91.5 GeV with the 90/60 optics.

where  $C$  is the LEP circumference and  $\Delta L_1$  is calculated from

$$\Delta L_1 = \sum D_x \delta. \quad (9)$$

The sum is over all correctors,  $D_x$  is the horizontal dispersion at the corrector, and  $\delta$  is the “kick”, i.e. the deflection due to the corrector. The calculated and measured values of  $D_x$  agree to within 2%, and the kick is known from the current in the corrector magnet. Figure 9 shows the evolution of  $\Delta L_1$  in physics for the 1997 LEP run. The size of the effect is somewhat larger than in previous years: for a large fraction of the run  $\Delta E$  reaches approximately 11 MeV. The contributions of the horizontal correctors to the beam energies measured by RD for the 90/60 and 60/60 optics differ by about 4 MeV at 45 GeV beam energy.

Recent simulations predict that the orbit corrector settings should *not* influence the central frequency by more than 0.5 Hz. This was confirmed by measurements made during the 1998 LEP run. Separate corrections for  $x_{\text{arc}}$  and for the energy shifts due to the horizontal corrector configurations are therefore applied.

The average beam energy shift from the orbit corrector settings is 6 MeV for the high energy running in 1997, which is much larger than in previous years. The 30% model uncertainty would imply an error of 2 MeV. This is increased to half of the total correction, 3 MeV, in view of the evolving understanding of the interplay of central frequency and orbit corrector effects.



## 5.5 Optics dependent effects

The majority of the RD measurements were made with the dedicated polarisation (60/60) optics, while the physics running was with the 90/60 optics. Both horizontal orbit corrector settings (see section 5.4) and current differences in the vertically and horizontally focussing quadrupoles can cause a difference of a few MeV between the beam energies with the two optics. These are accounted for by the corrections  $C_{\text{h.corr.}}$  and  $C_{\text{QFQD}}(t)$  in the model of the beam energy given by equation 3.

Simulations show that the overall energy difference can be of either sign, depending on the exact imperfections in the machine, and the difference is predicted to scale with the beam energy. The predicted difference at 45 GeV also has an uncertainty of 1.5 MeV from central frequency effects, described in section 5.2. The measured difference in the data is evaluated from the residuals  $E_{\text{pol}} - E_{\text{NMR}}$  with respect to the simultaneous fit to all RD measurements, using either optics. These can be seen in figure 2(a). The observed average beam energy difference between RD measurements with the two optics is:

$$E(90/60) - E(60/60) = +2 \text{ MeV at } 45 \text{ GeV.} \quad (10)$$

From the fill-to-fill scatter, the uncertainty on this measured difference is  $\leq 1$  MeV. Scaling the difference with the beam energy, a systematic uncertainty of 4 MeV is therefore taken to cover all uncertainties due to optics dependent effects at physics energy.

## 6 Evaluation of the centre-of-mass energy at each IP

As at LEP1, corrections to the centre-of-mass energy arise from the non-uniformity of the RF power distribution around LEP and from possible offsets of the beam centroids during collisions in the presence of opposite-sign vertical dispersion[1].

### 6.1 Corrections from the RF System

Since the beam energy loss due to synchrotron radiation is proportional to  $E_{\text{beam}}^4$ , operation of LEP2 requires a large amount of RF acceleration to maintain stable beam orbits. To provide this acceleration, new super-conducting (SC) RF cavities have been installed around all of the experiments in LEP. This implies that, contrary to LEP1, the exact anti-correlation of RF effects on the beam energy at IP4 and IP8 is no longer guaranteed, and that large local shifts in the beam energy can occur at any of the IPs. This also implies that the energy variation in the beams (the “sawtooth”) as they circulate around LEP is quite large (see figure 10.). This increases the sensitivity of the centre-of-mass energy to non-uniformities in the energy loss arising from differences in the local magnetic bend field, machine imperfections, etc.

The modelling of the energy corrections from the RF system is carried out by the iterative calculation of the stable RF phase angle  $\phi_s$  which proceeds by setting the total energy gain,  $V_{\text{tot}} \sin \phi_s$ , of the beams as they travel around the machine equal to all of the known energy losses. Here  $V_{\text{tot}}$  is the total RF accelerating voltage. The measured value of the synchrotron tune  $Q_s$  and the energy offsets between the beams as they enter and leave the experimental IPs are used to constrain energy variations due to overall RF voltage scale and RF phase errors. In particular, the phase error at each IP is set using

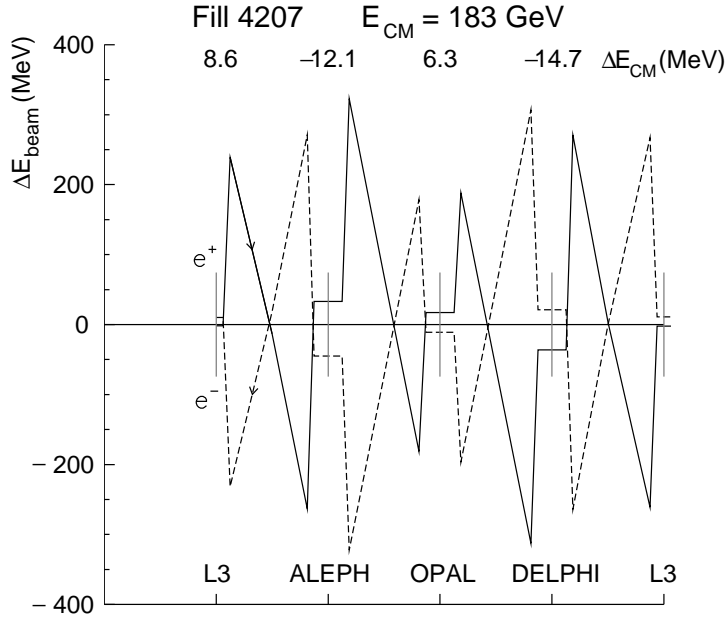


Figure 10: The evolution of the energy of each of the counter-rotating beams as they circulate in LEP, the so-called *energy sawtooth*. The electron beam is represented by the left-going dotted line, the positron beam by the right-going solid line. The light grey lines mark the positions of the IPs.  $\Delta E = 0$  denotes the average energy of LEP, i.e. that given by the rest of the energy model. The energy gains provided by the RF are clearly visible. This represents a typical RF configuration and centre-of-mass energy corrections for the 1997 running.  $\Delta E_{\text{CM}}$  is the shift in  $E_{\text{CM}}$  at each IP due to RF effects.

the size of the energy sawtooth measured by the LEP BOM system compared with the total RF voltage at that IP. This is a powerful constraint on potential phasing errors, as was seen in the LEP1 analysis.

The average corrections for the 1996 and 1997 running are shown in table 2. The corrections for running below the WW threshold are typically smaller by a factor of two, with correspondingly smaller errors. The bunchlet-to-bunchlet variation in corrections is negligible.

As at LEP1, the errors on the energy corrections are evaluated by a comparison of those quantities ( $Q_s$ , the orbit sawtooth, and the longitudinal position of the interaction point) which can be calculated in the RF model and can be measured in LEP. In addition, uncertainties from the inputs to the model, such as the misalignments of the RF cavities and the effects of imperfections in the LEP lattice, must also be considered. Since many of the uncertainties on the RF corrections scale with the energy loss in LEP, however, the overall uncertainty due to RF effects is larger at LEP2 than at LEP1. Note that the errors are given below in terms of  $E_{\text{beam}}$ , and are obtained by dividing the error on  $E_{\text{CM}}$  by two.

Comparison of the measured and calculated  $Q_s$  values reveals a discrepancy in the modelled and measured overall RF voltage seen by the beam. The difference is small, on the order of 4%, which can be explained by an overall scale error in the measured voltages or a net phase error in the RF system of a few degrees. An overall scale error changes the energy corrections by a corresponding amount (*i.e.*, a 10 MeV correction acquires

LEP IP	$\Delta E_{\text{CM}}$ (MeV)		
	$E_{\text{CM}} = 161$ GeV	$E_{\text{CM}} = 172$ GeV	$E_{\text{CM}} = 183$ GeV
2	19.7	18.8	8.1
4	-5.5	-5.8	-10.8
6	20.2	19.5	5.9
8	-9.3	-8.0	-13.3

Table 2: The average corrections (in MeV) to  $E_{\text{CM}}$  for each LEP IP and each energy point for the 1996 and 1997 RF models.

an error of 0.4 MeV, which is negligible), whereas phase errors can shift the energy by larger amounts at the IP closest to the error. For 1996, the overall error due to this mismatch was computed by assuming the entire phase error was localised to one side of an IP, and the largest shift taken as the error for all IPs (4 MeV  $E_{\text{beam}}$ ). For 1997, the total energy gain was normalised so that  $Q_s$  was correct, and the phase errors for each IP were calculated using the orbit measurement of the local energy gain. This resulted in a smaller error of 1.5 MeV on  $E_{\text{beam}}$  from the voltage scale and phasing effects.

The positions of all of the RF cavities in LEP have been measured repeatedly using a beam-based alignment technique with a systematic precision of 1 mm and a 1 mm rms scatter over time [10]. The systematic error on the energy corrections is evaluated by coherently moving the RF cavities in the model by 2 mm away from (towards) the IPs, and observing the change in  $E_{\text{CM}}$ . This results in a 1.5 MeV error on  $E_{\text{beam}}$  for 1996 and 1997.

Recently, a study of the effects of imperfections in the LEP lattice on the energy loss of the beams at LEP2 has been performed [11]. Calculations of the centre-of-mass energy in an ensemble of machines with imperfections similar to those of LEP yields an rms spread of 2.5 MeV  $E_{\text{beam}}$  in the predicted energy at the IPs due to non-uniformities in the energy loss of the beams. These shifts only depend on the misalignments and non-uniformities of all of the magnetic elements in LEP, which are essentially unmeasurable, and is not contained in any of the other error sources.

In order to keep the error estimate as conservative as possible, the error on the energy corrections from the RF should be considered 100% correlated between IPs and energy points. The total error from RF effects for each energy point is given in table 3.

## 6.2 Opposite sign vertical dispersion

In the bunch train configuration, beam offsets at the collision point can cause a shift in the centre-of-mass energy due to opposite sign dispersion [1]. The change in energy is evaluated from the calculated dispersion and the measured beam offsets from beam-beam deflection scans.

The dispersions have been calculated using MAD [12] for all the configurations in 1996 and 1997. No dedicated measurements of dispersion were made in 1996, while in 1997 the measured values agree with the prediction to within about 50%. This is the largest

cause of uncertainty in the possible correction. Beam offsets were controlled to within a few microns by beam-beam deflection scans. The resulting luminosity-weighted correction to the centre-of-mass energies are typically 1 to 2 MeV, with an error of about 2 MeV. No corrections have been applied for this effect, and an uncertainty of 2 MeV has been assigned.

## 7 Summary of systematic uncertainties

Source	Error [MeV]
Extrapolation from NMR-polarisation:	
NMR rms/ $\sqrt{N}$ at physics energy	10
Different $E_{\text{pol}}$ fills	5
Flux-loop test of extrapolation:	
NMR flux-loop difference at physics energy	20
Field not measured by flux loop	5
Polarisation systematic	1
$e^+e^-$ energy difference	2
Optics difference	4
Corrector effects	3
Tide	1
Initial dipole energy	2
Dipole rise modelling	1
IP specific corrections ( $\delta E_{\text{CM}}/2$ ):	
RF model	4
Dispersion	2
Total	25

Table 3: Summary of contributions to the 1997 beam energy uncertainty.

The contributions from each source of uncertainty described above are summarised in table 3. The first groups describe the uncertainty in the normalisation derived from NMR-polarisation comparisons, NMR-flux-loop tests and the part of the bending field not measured by the flux-loop. These extrapolation uncertainties dominate the analysis. The subsequent errors concern the polarisation measurement, specifically its intrinsic precision (which is less than 1 MeV), the possible difference in energy between electrons and positrons, and the difference between optics. None of the additional uncertainties from time variations in a fill, and IP specific corrections contribute an uncertainty greater than 5 MeV.

## 7.1 Uncertainty for data taken in 1996

The analysis of the 1996 data was largely based on a single fill with RD measurements at 45 and 50 GeV. The apparent consistency of the flux-loop and NMR data compared to RD data was about 2 MeV over this 5 GeV interval, i.e. a relative error  $4 \times 10^{-4}$ , which using a naive linear extrapolation would give an uncertainty of 13.5 (15) MeV at 81.5 (86) GeV. These errors were inflated to 27 (30) MeV before the 1997 data were available, since there was no test of reproducibility from fill to fill, there was no check of the non-linearity possible from a fill with two energy points, and the field outside the flux loop had not been studied. Although more information is available in 1997, this larger uncertainty is retained for the 1996 data, partly motivated by the sparsity of RD measurements in that year. In addition, the single parameter fit that was used for 1996 leads to a shift of 20 MeV, and an increased scatter of 60 MeV, when used to predict the energies in physics in 1997.

The uncertainties for the two 1996 data samples can be assumed to be fully correlated. However, the extrapolation uncertainty for the 1997 data is somewhat better known. Since the energy difference between the maximum RD energy and the physics energy is nearly the same in the two years, it can be assumed that the 25 MeV uncertainty of 1997 data is common to the 1996 data.

## 7.2 Lower energy data taken in 1996 and 1997

During 1996 and 1997, LEP also operated at the Z resonance, to provide data samples for calibrating the four experiments, and at intermediate centre-of-mass energies, 130–136 GeV, to investigate effects seen at the end of 1995 at “LEP 1.5”. The dominant errors on the beam energy are from the extrapolation uncertainty, and scale with the difference between physics energy and RD energy. The optics difference scales in the same way. Several other effects such as the tide correction are proportional to the beam energy. The dipole rise per fill depends in addition on whether bend modulation was carried out at the start of fill. The total beam energy uncertainties are found to be 6 MeV for Z running, and 14 MeV for LEP 1.5 running.

## 8 Centre-of-mass energy spread

The spread in centre-of-mass energy is relevant for evaluating the width of the W boson, which is about 2 GeV. The beam energy spread can be predicted for a particular optics, beam energy and RF frequency shift. This spread has been calculated for every 15 minutes of data taking, or more often in the case of an RF frequency shift. Weighting the prediction by the (DELPHI) integrated luminosity gives the average “predicted” values in table 4 for each nominal centre-of-mass energy. Overall averages for all data taken close to 161, 172 and 183 GeV are also listed. The error in the prediction is estimated to be about 5%, from the differences observed when a quantum treatment of radiation losses is implemented.

The beam energy spread can also be derived from the longitudinal bunch size measured by one of the experiments. This procedure has been applied to the longitudinal size of the interaction region measured in ALEPH,  $\sigma_z^{\text{ALEPH}}$ , which is related to the energy spread

Year	$E_{\text{CM}}$ [GeV]	$\mathcal{L}$ [pb $^{-1}$ ]	$\sigma_{E_{\text{beam}}}$ [MeV]	
			Predicted	Derived
1996	161.3	10	$102 \pm 5$	$105 \pm 1 \pm 5$
	164.5	0.05	$106 \pm 5$	$97 \pm 35 \pm 4$
All “161”			$102 \pm 5$	$105 \pm 5$
	170.3	1	$115 \pm 6$	$125 \pm 4 \pm 4$
	172.3	9	$117 \pm 6$	$111 \pm 1 \pm 4$
All “172”			$117 \pm 6$	$113 \pm 4$
1997	130.0	3	$66 \pm 3$	$71 \pm 1 \pm 4$
	136.0	3	$74 \pm 4$	$80 \pm 1 \pm 4$
	180.8	0.2	$141 \pm 7$	$106 \pm 14 \pm 3$
	182.0	6	$164 \pm 8$	$146 \pm 5 \pm 5$
	182.7	46	$154 \pm 8$	$154 \pm 6 \pm 6$
	183.8	2	$145 \pm 7$	$124 \pm 4 \pm 6$
All “183”			$155 \pm 8$	$152 \pm 8$

Table 4: Beam energy spreads. Note that these should be multiplied by  $\sqrt{2}$  to give the centre-of-mass energy spread. The predicted values, and the values derived from the bunch length measurement are given, together with the approximate luminosity,  $\mathcal{L}$ , recorded at each nominal centre-of-mass energy. Luminosity weighted predictions for all fills with centre-of-mass energy close to 161, 172 and 183 GeV are also given.

by [1, 13]:

$$\sigma_{E_{\text{beam}}} = \frac{\sqrt{2}E_{\text{beam}}}{\alpha R_{\text{LEP}}} Q_s \sigma_z^{\text{ALEPH}}. \quad (11)$$

The momentum compaction factor  $\alpha$  is known for each optics,  $R_{\text{LEP}}$  is the average radius of the LEP accelerator, and  $Q_s$  is the incoherent synchrotron tune. This is derived from the measured coherent  $Q_s$  using:

$$\frac{Q_s^{\text{coh}}}{Q_s^{\text{incoh}}} = 1 - \kappa \frac{I^{\text{bunch}}}{300 \mu\text{A}} \quad (12)$$

The parameter  $\kappa$  was measured in 1995 to be  $0.045 \pm 0.022$  at the Z. For the same  $Q_s$  and machine configuration, this would scale with  $1/E_{\text{beam}}$ . This scaling has been used for the central values of  $\sigma_{E_{\text{beam}}}$  evaluated from the measured bunch lengths in table 4. However, the reduction in the number of copper RF accelerating cavities in the machine since 1995 is expected to further reduce the value of  $\kappa$ , so the uncertainty of  $\pm 0.022$  is retained for all energies. The value and uncertainty are consistent with estimates from the variation of bunch length with current measured with the streak camera<sup>2</sup> in 1998. Where two errors are quoted for the derived number, they are the statistical uncertainty in the bunch length measurement, and a systematic uncertainty, which is dominated by the uncertainty in  $\kappa$ ,

<sup>2</sup>The streak camera measures the bunch length parasitically by looking at synchrotron light emitted when the bunch goes through a quadrupole or wiggler magnet.

with a 1 MeV contribution from the uncertainty in  $\alpha$ . The predicted and derived values agree well within the quoted errors.

The measurement of  $Q_s$  is difficult for high energy beams, and in 1997, a reliable value is only available for 58% of the data. It is therefore recommended to use the predicted values. The beam energy spreads must be multiplied by  $\sqrt{2}$  to give the centre-of-mass energy spreads [1, 13], which are:  $144 \pm 7$  MeV at 161 GeV,  $165 \pm 8$  MeV at 172 GeV and  $219 \pm 11$  MeV at 183 GeV.

## 9 Conclusions and outlook

The method of energy calibration by magnetic extrapolation of resonant depolarisation measurements at lower energy has made substantial progress with the 1997 data. The success in establishing polarisation above the Z has allowed a robust application of the method, and the mutual consistency of the resonant depolarisation, NMR and flux-loop data has been established at the 20 MeV level at physics energy, with a total systematic uncertainty in the beam energy of 25 MeV. The precision is limited by the understanding of the NMR/flux-loop comparison.

As LEP accumulates more high energy data, the experiments themselves will be able to provide a cross-check on the centre-of-mass energy by effectively measuring the energy of the emitted photon in events of the type  $e^+e^- \rightarrow Z\gamma \rightarrow f\bar{f}\gamma$ , where the Z is on-shell. This can be done using a kinematic fit of the outgoing fermion directions and the precisely determined Z-mass from LEP1. The ALEPH collaboration have shown[14] the first attempt to make this measurement in the  $q\bar{q}\gamma$  channel, where they achieve a precision of  $\delta E_{\text{beam}} = \pm 110(\text{stat}) \pm 53(\text{syst})$  MeV. With 500 pb<sup>-1</sup> per experiment, the statistical precision on this channel should approach 15 MeV. Careful evaluation of systematic errors will determine the usefulness of this approach.

In future, a new apparatus will be available for measuring the beam energy. The LEP Spectrometer Project [15] will measure the bend angle of the beams using standard LEP beam pick ups with new electronics to measure the position to the order of a micron precision as they enter or leave a special dipole in the LEP lattice whose bending field has been surveyed with high precision. A first phase of the spectrometer is already in place for the 1998 running, with the aim of checking the mechanical and thermal stability of the position measurement. In 1999, the new magnet will be installed, and the aim is to use this new, independent method to measure the beam energy to 10 MeV at high energy. It should be possible to propagate any improvement in the beam energy determination back to previous years by correcting the extrapolation and correspondingly reducing the uncertainty.

## Acknowledgements

The unprecedented performance of the LEP collider in this new high energy regime is thanks to the SL Division of CERN. In particular, careful work and help of many people in SL Division has been essential in making specific measurements for the energy calibration.

We also acknowledge the support of the Particle Physics and Astronomy Research Council, UK.

## References

- [1] “Calibration of centre-of-mass energies at LEP1 for precise measurements of Z properties”, LEP Energy Working Group, Eur. Phys. J. C 6 (1999) 2, 187-223.
- [2] See for example papers by H. Przysiezniak and M. Thomson, ICHEP98, Vancouver, Canada, 22-29 July 1998.
- [3] B. Dehning et al., “Dynamic beam based calibration of beam position monitors”, CERN-SL-98-038-BI, June 1998. Presented at 6th European Particle Accelerator Conference (EPAC 98), Stockholm, Sweden, 22-26 June 1998.
- [4] J. A. Uythoven, “A LEP (60,60) Optics for Energy Calibration Measurements”, CERN-SL-97-058-OP.
- [5] See for example B. Dehning in the proceedings of the 8th LEP Performance Workshop, Chamonix, 1998, CERN-SL-98-006 DI.
- [6] R. Bailey et al., “LEP Energy Calibration”, Proc. of the 2nd EPAC, Nice, France (1990) and CERN SL/90-95.  
H. Schmickler, “Measurement of the Central Frequency of LEP”, CERN SL-MD note 89 (1993).
- [7] J. Wenninger, “Radial Deformations of the LEP ring”, CERN SL / Note 95-21 (OP).  
J. Wenninger, “Measurement of Tidal Deformations of the LEP Ring with Closed Orbits”, SL-Note 96-22 (OP).
- [8] J. Wenninger, “Orbit Corrector Magnets and Beam Energy”, SL-Note 97-06 OP.
- [9] LEP Design Report Vol. III, LEP2, CERN-AC/96-01(LEP2).
- [10] LEP Energy Working Group Note 97-03, “A Systematic Check of SC Cavity Alignment Using LEP Beams”, M.D. Hildreth.
- [11] J.M. Jowett, “Monte-Carlo Study of the (102°, 90°) Physics Optics for LEP”, SL-Note-97-84 AP.
- [12] H. Grote and F.C. Iselin, “The MAD program”, version 8.16, CERN SL/90-13 (AP) (rev.4, March 19, 1995)
- [13] LEP Energy Working Group Note 96-07, “Determination of the LEP Energy Spread Using Experimental Constraints”, E. Lançon and A. Blondel.
- [14] The ALEPH Collaboration, “Preliminary Evaluation of the LEP Centre-of-Mass Energy Using  $Z\gamma$  Events”, Contributed paper 1038 to ICHEP98, Vancouver, Canada, 22-29 July 1998.
- [15] See for example M. Placidi in the proceedings of the 8th LEP Performance Workshop, Chamonix, 1998, CERN-SL-98-006 DI.